Surface-Coil MR of Orbital Pseudotumor

Scott W. Atlas[1]
Robert I. Grossman[1]
Peter J. Savino[2]
Robert C. Sergott[2]
Norman J. Schatz[2]
Thomas M. Bosley[2]
David B. Hackney[1]
Herbert I. Goldberg[1]
Larissa T. Bilaniuk[1]
Robert A. Zimmerman[1]

Fifteen patients with clinical presentations compatible with idiopathic inflammatory orbital pseudotumor were examined by CT and MR imaging to determine if MR could add specificity to the CT appearance of this entity. MR was performed on a 1.5 T system, using surface-coil and head-coil techniques. Idiopathic pseudotumor was confirmed in nine patients on the basis of response to steroid therapy in the absence of local cause or systemic illness. One other patient had biopsy-proven idiopathic pseudotumor. Five patients proved to have other orbital entities, including metastases, infectious myositis, hemorrhage, and orbital sarcoid. In all 10 patients with confirmed pseudotumor, CT and MR were abnormal. MR abnormalities in 10 of 10 patients with pseudotumor were hypointense to fat and isointense to muscle on T1-weighted images. On T2-weighted images the lesions of pseudotumor were isointense or only minimally hyperintense to fat in nine of 10 cases; in one case, the enlarged muscle was markedly hyperintense to fat. The MR signal intensity of pseudotumor was similar to that found in infectious myositis and sarcoid. These findings contrasted to the MR appearance of the other disease entities examined. Metastases appeared markedly hyperintense to fat on T2-weighted images, while hematoma was hyperintense to muscle and isointense to fat on T1-weighted images and markedly hyperintense to fat on T2-weighted images. In our preliminary series, surface-coil MR appears to add specificity to the CT appearance of orbital pseudotumor.

Pseudotumor of the orbit often presents with painful ophthalmoparesis and proptosis; however, clinical manifestations can vary, and pain may be minimal or absent [1–3]. Because CT of orbital pseudotumor may appear identical to other entities, including infiltrative malignancies (i.e., lymphoma or metastases) [4–6], increased specificity with noninvasive imaging is highly desirable. We examined 15 patients with a clinical presentation compatible with orbital pseudotumor on a 1.5 T MR scanner, using both surface and head coils. This report describes the MR findings in 10 patients with clinically or pathologically confirmed orbital pseudotumor. An additional five patients had similar clinical manifestations but proved to have other orbital disease. The MR appearance of these two groups are compared.

Subjects and Methods

Ten patients, ranging in age from 11–74 years, with the eventual clinical diagnosis of idiopathic orbital pseudotumor confirmed by clinical course and response to steroid therapy (nine of 10 patients) or biopsy (one of 10 patients) in the absence of local cause or systemic disease, underwent CT and MR. Five additional patients who presented with clinical manifestations consistent with pseudotumor were examined with similar MR techniques and found to have other orbital diseases. CT was performed on a General Electric 9800 scanner, and in nine patients images were obtained after intravenous bolus infusion of 50 ml of 60% meglumine diatrizoate, followed by a drip infusion of 300 ml of 30% meglumine diatrizoate. In one patient, CT was performed without intravenous contrast. CT section thickness was 3 mm in the axial plane and 5 mm in the coronal plane. MR was performed on a General Electric 1.5 T Signa system, using spin-echo techniques. During surface-coil imaging, the transmitter

This article appears in the January/February 1987 issue of *AJNR* and the April 1987 issue of *AJR*.

Received April 23, 1986; accepted after revision July 30, 1986.

Presented at the annual meeting of the American Society of Neuroradiology, San Diego, January 1986.

[1] Department of Radiology, Hospital of the University of Pennsylvania, 3400 Spruce St., Philadelphia, PA 19104. Address reprint requests to R. I. Grossman.

[2] Neurophthalmology Service, Wills Eye Hospital, 9th and Walnut Sts., Philadelphia, PA 19107.

***AJNR* 8:141–146, January/ February 1987**
0195–6108/87/0801–0141

coil was a 55-cm diameter cylindrical coil, routinely used for body imaging. The receiving coil, a mask-configuration surface coil measuring 9 cm in height and 14 cm in width, was placed on the patient's face, overlying the orbits. T2-weighted images were obtained by using a 28-cm diameter head coil as receiver and transmitter in 13 of 15 cases. Surface-coil images were 3 mm thick. Head-coil images were 3–5 mm thick. All MR images had interslice gaps of 50% of the section thickness. Images were obtained in the axial, coronal, and/or sagittal planes. T1-weighted images were obtained with repetition time (TR) = 600 msec and echo time (TE) = 20–25 msec. T2-weighted images were obtained with TR = 2000–2500 msec and TE = 80 msec. All MR images used a 128 × 256 matrix and two excitations. T1-weighted images required 2 min 35 sec of scanning time, while T2-weighted images required 8 min 38 sec to 10 min 48 sec.

In our experience, when imaging the orbit with a surface coil, globe motion significantly degrades image quality. To minimize this problem, patients were asked to keep their eyes open and fix their gaze upon a single spot during MR performed with the surface coil. When imaging with the head coil or during CT, patients were simply told to relax, since in our experience images obtained with these techniques do not suffer degradation from globe motion.

Technicians photographing orbital MR images were instructed to use a somewhat wider window width than usual for T1-weighted images in order to unmask potentially subtle retrobulbar lesions that might otherwise be obscured by the marked hyperintensity of orbital fat.

Results

In all 10 patients with the confirmed diagnosis of idiopathic orbital pseudotumor, CT and MR were abnormal. Eight patients had unilateral findings, and two patients had bilateral abnormalities. Surface-coil T1-weighted images depicted all of the CT findings and provided the finest anatomic definition. Motion artifacts were variably present, depending on the patient's ability to fix his or her gaze for the required scanning time. Characteristic findings on T1-weighted images included either focal or diffuse regions of decreased signal intensity, as compared with orbital fat (isointense to extraocular muscle), seen in all 10 patients (Figs. 1C, 1D, and 2B). Orbital fat had a decrease in signal intensity on T1-weighted images when compared with the normal contralateral side in two patients (Fig. 3). In two other patients, the orbital fat appeared to have decreased signal intensity when compared with the uninvolved side; however, artifactual intensity gradients from asymmetric coil position were actually responsible for this factitious finding.

Uveal-scleral thickening was clearly demonstrated in two patients (Fig. 2). Enlargement of extraocular muscle(s) was present in seven patients; the muscle insertions were involved in three patients (Fig. 1). In nine patients, T2-weighted images showed all lesions to be isointense, or minimally hyperintense, to orbital fat. In one patient, T2-weighted images showed a markedly hyperintense enlarged medial rectus muscle. Surface-coil T2-weighted images were usually markedly degraded by globe and patient motion, because over 10 min is required for scanning with TR = 2500 msec and because a surface coil is more susceptible to motion artifact. Head-coil images with T2 weighting were usually not significantly degraded by motion; thicker sections, however, were necessary

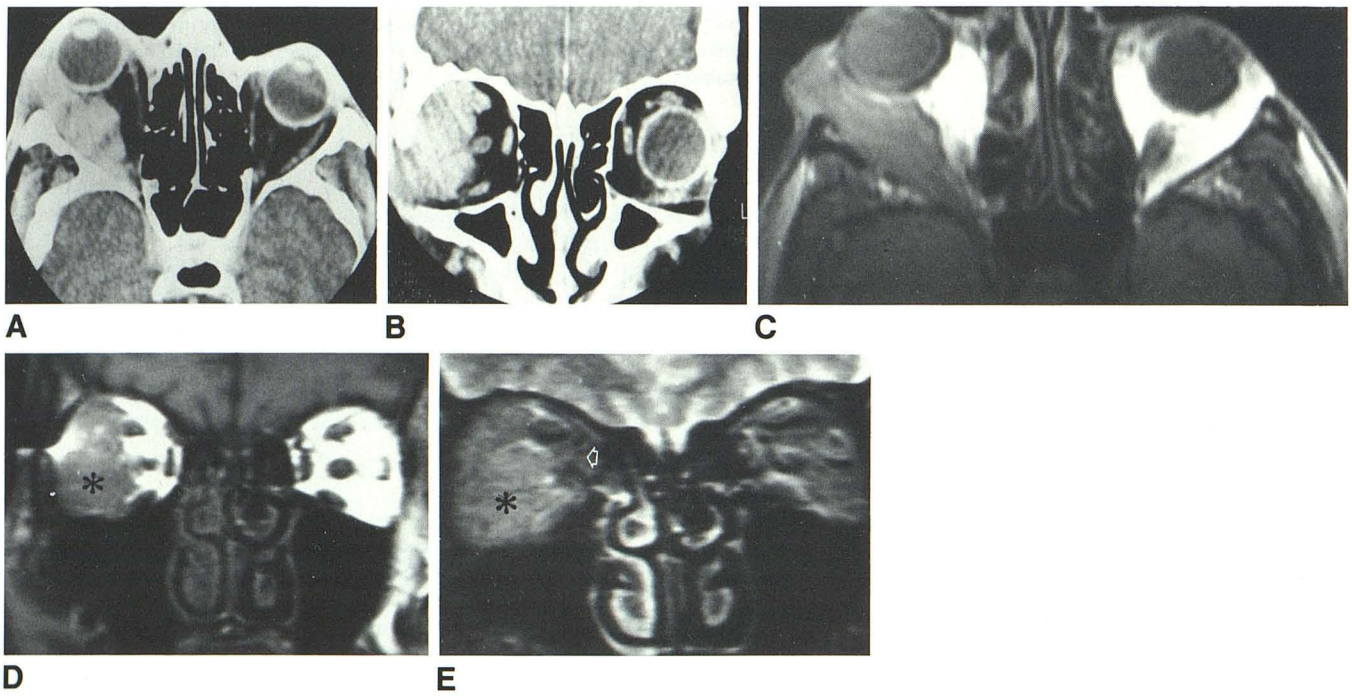

Fig. 1.—Myositic pseudotumor.

***A*, Axial CT.**

***B*, Coronal CT. Note large, enhancing mass involving right lateral rectus muscle and its insertion extending into lacrimal fossa.**

***C*, Axial surface-coil MR, T1-weighted image (TR = 600 msec, TE = 25 msec).**

***D*, Coronal surface-coil MR, T1-weighted image (TR = 600 msec, TE = 25 msec). Right lateral rectus mass (*asterisk*) is isointense to muscle, hypointense to orbital fat.**

***E*, Coronal head-coil MR, T2-weighted image (TR = 2500 msec, TE = 80). The mass (*asterisk*) is approximately isointense to orbital fat (*arrow*).**

Fig. 2.—Orbital pseudotumor with uveal-scleral thickening.
A, Axial CT shows bilateral, enhancing uveal-scleral thickening (*arrows*).
B, Axial surface-coil MR, T1-weighted image (TR = 600 msec, TE = 25 msec). MR clearly defines bilateral uveal-scleral thickening (*arrows*), which is isointense to muscle, hypointense to orbital fat.
C, Axial surface-coil MR, T2-weighted image (TR = 2000, TE = 80). The regions of uveal-scleral thickening (*arrowheads*) are only minimally hyperintense to orbital fat.

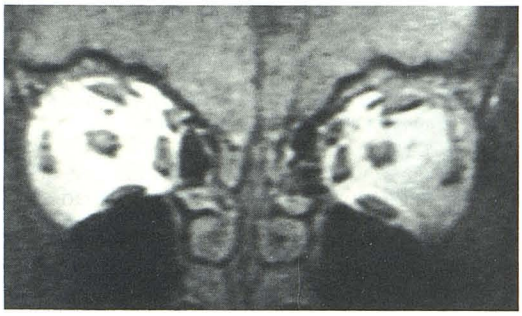

Fig. 3.—Orbital pseudotumor with hypointense orbital fat. Coronal surface-coil MR, T1-weighted image (TR = 600 msec, TE = 20 msec). Note diffusely decreased signal intensity of orbital fat on affected left side as compared with normal fat in contralateral orbit.

TABLE 1: **Signal Intensity Relative to Fat and Muscle**

	To Fat		To Muscle	
	T1 Weighted	T2 Weighted	T1 Weighted	T2 Weighted
Pseudotumor (9/10)	↓	→	→	→
Infectious myositis (1)	↓	→	→	→
Sarcoid (1)	↓	→	→	→
Metastases (2)	↓	↑	→	↑
Hemorrhage (1)	→	↑	↑	↑

Note.—↓ = hypointense; → = isointense; ↑ = hyperintense.

(to compensate for the lower signal-to-noise ratio), thereby limiting spatial resolution.

Five patients with pseudotumorlike presentations had other orbital pathology, including spontaneous retrobulbar hemorrhage, orbital metastases (two), infectious orbital myositis secondary to adjacent subperiosteal abscess, and orbital sarcoid (Table 1). In one patient with painful ophthalmoplegia, idiopathic retrobulbar hemorrhage was definitively diagnosed as a result of both T1- and T2-weighted images that showed an enlarged inferior rectus muscle with central hyperintensity (relative to muscle) (Fig. 4).

In a patient with known, widely metastatic breast carcinoma, MR demonstrated an extraconal mass hypointense to orbital fat on T1-weighted images. On T2-weighted images, the mass was markedly hyperintense as compared with orbital fat (Fig. 5). In another patient with biopsy-proven metastatic breast carcinoma, T1-weighted images demonstrated bilateral retrobulbar masses involving extraocular muscles that were hypointense to fat. T2-weighted images showed that these masses were markedly hyperintense to fat (Fig. 6).

In one patient with sarcoidosis (diagnosed on the basis of classic bilateral hilar and right paratracheal adenopathy on chest radiograph in the absence of symptoms) MR demonstrated bilateral intraconal masses that encased the posterosuperior aspect of the globes and extended into the lacrimal fossae (Fig. 7). T1-weighted images with the surface coil demonstrated hypointense (to fat) infiltrative masses. Head-coil T2-weighted images revealed isointensity (to fat) in these regions.

Infectious orbital myositis secondary to adjacent subperiosteal abscess on MR demonstrated hypointensity on T1-weighted images and isointensity (to fat) on T2-weighted images.

Discussion

Orbital pseudotumor is usually a clinical diagnosis, although unusual presentations often require radiographic evaluation and, occasionally, biopsies [7–9]. CT, however, is often nonspecific [4–6]. A-mode orbital sonography may also be useful in evaluating pseudotumor [6, 10], both as a rapid screening technique and as a method of delineating surface characteristics and, to some extent, tissue characteristics. Sonography may add specificity to the radiographic appearance of some retrobulbar masses, but it is markedly operator-dependent. MR, including surface-coil techniques, has been useful in a variety of orbital disease entities [11, 12]. In our study, orbital

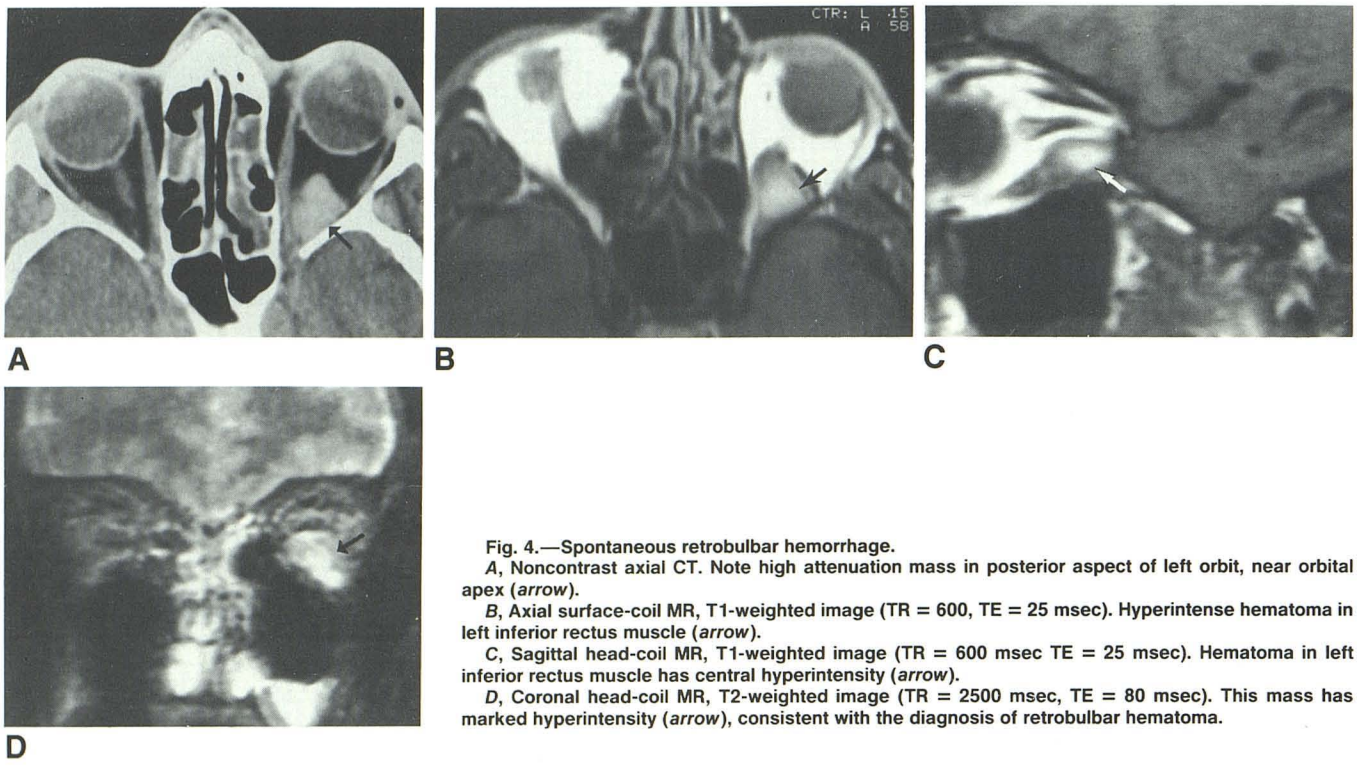

Fig. 4.—Spontaneous retrobulbar hemorrhage.
A, Noncontrast axial CT. Note high attenuation mass in posterior aspect of left orbit, near orbital apex (*arrow*).
B, Axial surface-coil MR, T1-weighted image (TR = 600, TE = 25 msec). Hyperintense hematoma in left inferior rectus muscle (*arrow*).
C, Sagittal head-coil MR, T1-weighted image (TR = 600 msec TE = 25 msec). Hematoma in left inferior rectus muscle has central hyperintensity (*arrow*).
D, Coronal head-coil MR, T2-weighted image (TR = 2500 msec, TE = 80 msec). This mass has marked hyperintensity (*arrow*), consistent with the diagnosis of retrobulbar hematoma.

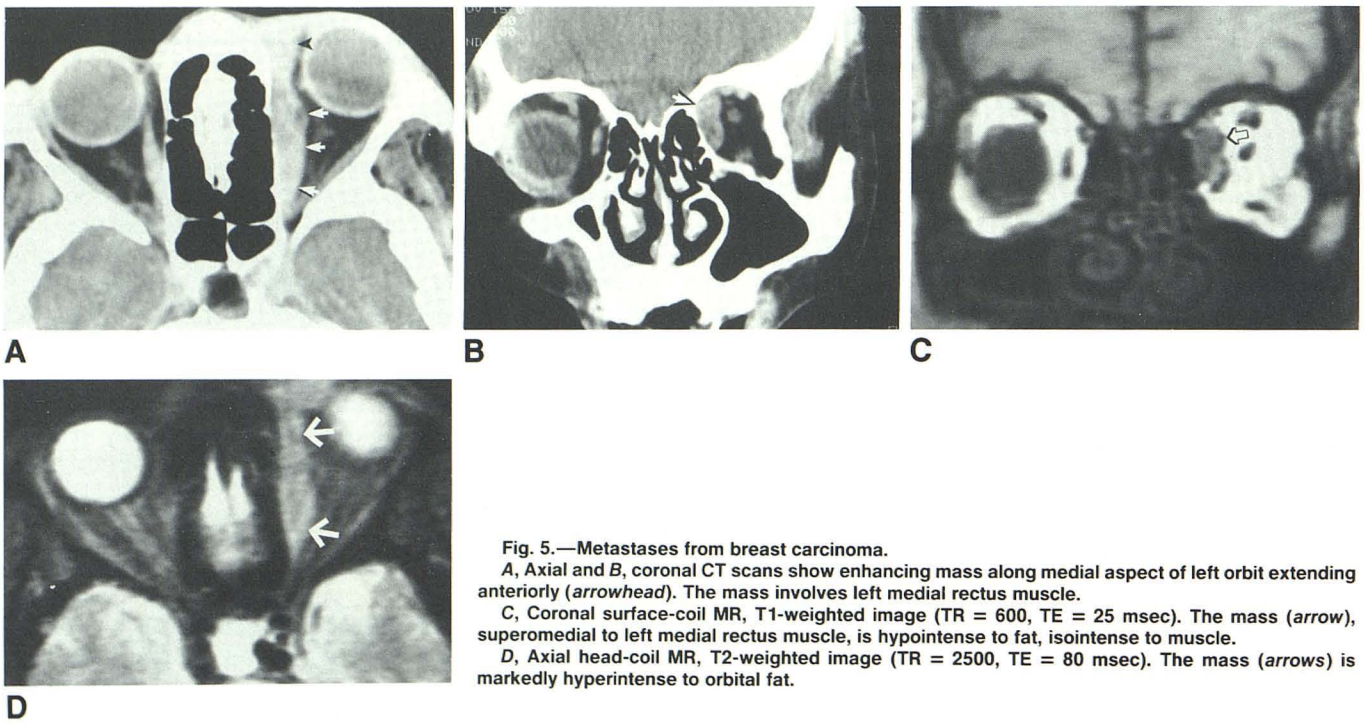

Fig. 5.—Metastases from breast carcinoma.
A, Axial and *B*, coronal CT scans show enhancing mass along medial aspect of left orbit extending anteriorly (*arrowhead*). The mass involves left medial rectus muscle.
C, Coronal surface-coil MR, T1-weighted image (TR = 600, TE = 25 msec). The mass (*arrow*), superomedial to left medial rectus muscle, is hypointense to fat, isointense to muscle.
D, Axial head-coil MR, T2-weighted image (TR = 2500, TE = 80 msec). The mass (*arrows*) is markedly hyperintense to orbital fat.

pseudotumor appeared on T1-weighted images as hypointense to orbital fat (isointense to muscle) in all cases. On T2-weighted images, lesions were isointense or only minimally hyperintense to orbital fat in nine of 10 cases. Other benign inflammatory entities (infectious myositis and sarcoid) had identical signal-intensity patterns. This appearance contrasted to other disease entities, including malignancy and hematoma, which appeared markedly hyperintense (to fat) on T2-weighted images. Furthermore, the retrobulbar intramuscular hematoma appeared hyperintense to muscle (isointense to

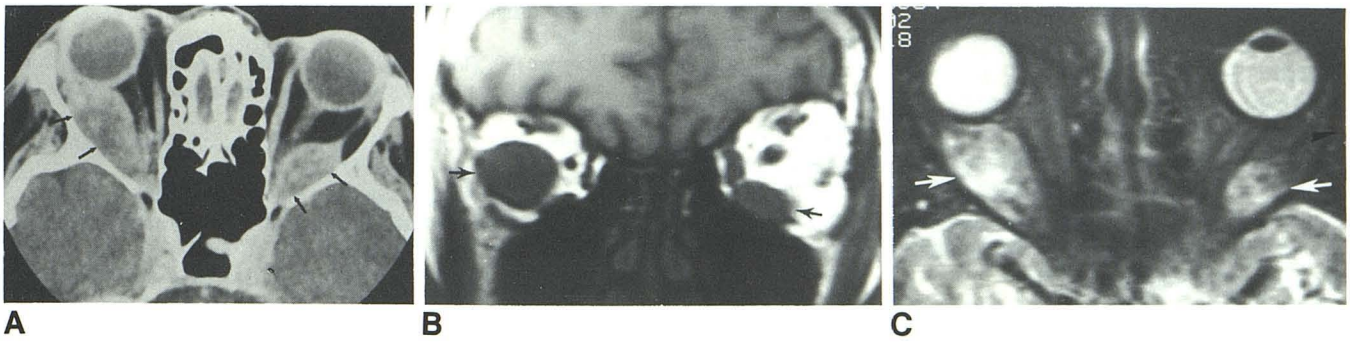

Fig. 6.—Metastases from breast carcinoma.
A, Axial CT shows bilateral masses involving rectus muscles (*arrows*). Note inhomogeneous low attenuation of these masses.
B, Coronal surface-coil MR, T1-weighted image (TR = 600, TE = 20 msec). Masses (*arrows*) are hypointense to fat and isointense to muscle.
C, Axial head-coil MR, T2-weighted image (TR = 2500, TE = 80 msec). Note marked hyperintensity of masses (*arrows*) as compared with orbital fat.

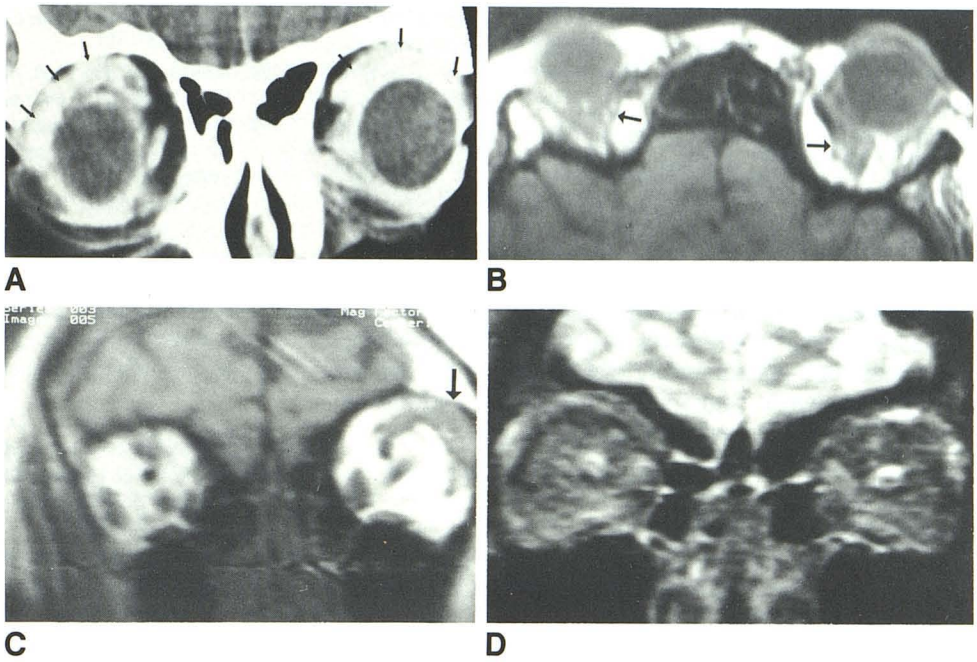

Fig. 7—Orbital sarcoid.
A, Coronal CT. Bilateral masses encircle superolateral aspect of globes (*arrows*).
B, Axial surface-coil MR, T1-weighted image (TR = 600, TE = 25 msec).
C, Coronal surface-coil MR, T1-weighted image (TR = 600, TE = 25 msec). Note bilateral retrobulbar masses that encase posterosuperior aspects of both globes and extend into left lacrimal fossa (*arrow*). These masses are hypointense to fat, isointense to muscle.
D, Coronal head-coil MR, T2-weighted image (TR = 2500, TE = 80 msec). The masses are approximately isointense to orbital fat.

fat) on T1-weighted images, indicating its hemorrhagic nature [13]. The cause of the apparent differences in signal-intensity characteristics of idiopathic pseudotumor and similar benign inflammatory orbital conditions from malignancy are uncertain; the degree of cellularity versus free-water content of the lesion may account for this discrepancy, but this is only speculation. MR appears to add specificity to the CT appearance of orbital pseudotumor, and may aid in differentiating benign from some malignant lesions. Preliminary reports on orbital MR by some authors have also suggested this, while others have disagreed [14–20].

Orbital MR is not without pitfalls. MR of orbital disease, in comparison to CT, has been limited by poor spatial resolution related to section thickness. Reduction in section thickness results in a lower signal-to-noise ratio [21]. Increasing scanning time, in an effort to improve the signal-to-noise ratio, is undesirable in orbital MR, because patients must fix their gaze for the entire scanning time. The resultant motion artifacts severely degrade image quality. However, the use of surface coils and high field strength may improve the signal-to-noise ratio [11, 12, 21], thereby allowing thinner sections without concomitantly increasing imaging time. Surface-coil MR is extremely operator-, patient-, and photographer-dependent. A surface coil positioned asymmetrically can result in severe signal-intensity gradients. In addition, since signal drop-off is significant as the distance of the area of interest from the surface coil increases, comparison of lesion signal intensities to nearby structures (i.e., fat) may be difficult. T1- and T2-weighted images are required for MR diagnosis; however, T2-weighted images obtained with the head coil appeared to be less degraded by artifact than those obtained with the surface coil. Such imaging techniques limit the potential spatial resolution. Patient cooperation is a prerequisite for successful surface-coil imaging of the orbit. Any lack of

cooperation makes the study essentially worthless, which is why surface-coil imaging is often inappropriate for young children. Sedation is not useful, as involuntary globe motion is significant in the sedated patient. The images are also photographer-dependent. The technique of photographing retrobulbar abnormalities on MR requires a certain level of expertise and sophistication, as an improperly windowed image can mask subtle lesions in the high signal intensity of orbital fat. Additionally, bony involvement with orbital disease is not well delineated with MR.

From our experience, we suggest the following techniques for MR of the orbit. T1-weighted images should be performed with surface-coil imaging. High-resolution scans can be obtained with 3-mm thin sections without increasing the number of excitations (which would increase scanning time). Both axial and coronal images should be obtained in all cases. Sagittal imaging may be helpful for perioptic/optic nerve lesions, orbital apex lesions, and abnormalities involving the superior and inferior rectus muscles. When imaging with the surface coil, the patient should be instructed to keep his eyes open and fix his gaze in one direction for the entire scan time. Particular attention should be made to coil positioning to avoid intensity gradients. T2-weighted images, which require long TR and long TE, necessitate, in our experience, the use of the head coil to avoid severe image degradation by motion artifact in most cases. Five-millimeter sections are usually adequate to display signal-intensity abnormalities.

In summary, surface-coil MR of orbital pseudotumor has added to the specificity of radiographic diagnosis when compared with CT. Lesions are clearly delineated on both imaging techniques, but signal-intensity characteristics on MR may distinguish between hemorrhage, malignancy, and pseudotumor (or other benign inflammation).

REFERENCES

1. Blodi FC, Gass JDM. Inflammatory pseudotumor of the orbit. *Br J Ophthalmol* **1968**;52:79–93
2. Nugent RA, Rootman J, Robertson WD, Lapointe JS, Harrison PB. Acute orbital pseudotumors: classification and CT features. *AJR* **1981**;137:957–962
3. Rootman J, Nugent R. The classification and management of acute orbital pseudotumors. *Ophthalmology* **1982**;89:1040–1048
4. Dresner SC, Rothfus WE, Slamovits TL, Kennerdell JS, Curtin HD. Computed tomography of orbital myositis. *AJR* **1984**;143:671–674
5. Rothfus WE, Curtin HD. Extraocular muscle enlargement: a CT review. *Radiology* **1984**;157:677–681
6. Balchunas WR, Quencer RM, Byrne SF. Lacrimal gland and fossa masses: evaluation by computed tomography and A-mode echography. *Radiology* **1983**;149:751–758
7. Sergott RC, Glaser JS, Charyulu K. Radiotherapy for idiopathic inflammatory pseudotumor; indications and results. *Arch Ophthalmol* **1981**;99:853–856
8. Leone CR Jr, Lloyd WC III. Treatment protocol for orbital inflammatory disease. *Ophthalmology* **1985**;92:1325–1331
9. Kennerdell JS, Johnson BL, Deutsch M. Radiation treatment of orbital lymphoid hyperplasia. *Ophthalmology* **1979**;86:942–947
10. Byrne SF, Glaser JS. Orbital tissue differentiation with standardized echography. *Ophthalmology* **1983**;90:1071–1090
11. Bilaniuk LT, Schenck JF, Zimmerman RA, et al. Ocular and orbital lesions: surface coil MR imaging. *Radiology* **1985**;156:669–674
12. Schenck JF, Hart HR, Foster TH, et al. Improved MR imaging of the orbit at 1.5 T with surface coil. *AJNR* **1985**;6:193–196
13. Gomori JM, Grossman RI, Goldberg HI, Zimmerman RA, Bilaniuk LT. Intracranial hematomas: imaging by high-field MR. *Radiology* **1985**;157:87–93
14. Char DH, Sobel D, Kelly WM, Kjos BO, Norman D. Magnetic resonance scanning in orbital tumor diagnosis. *Ophthalmology* **1985**;92:1305–1310
15. Edwards JH, Hyman RA, Vacirca SJ, et al. 0.6 T magnetic resonance imaging of the orbit. *AJNR* **1985**;6:253–258
16. Sobel DF, Kelly W, Kjos BO, Char D, Brant-Zawadzki M, Norman D. MR imaging of orbital and ocular disease. *AJNR* **1985**;6:259–264
17. Sobel DF, Mills C, Char D, et al. NMR of the normal and pathologic eye and orbit. *AJNR* **1984**;5:345–350
18. Hawkes RC, Holland GN, Moore WS, Rizk S, Worthington BS, Kean M. NMR imaging in the evaluation of orbital tumors. *AJNR* **1983**;4:254–256
19. Moseley I, Brant-Zawadzki M, Mills C. Nuclear magnetic resonance imaging of the orbit. *Br J Ophthalmol* **1983**;67:333–342
20. Han JS, Benson JE, Bonstelle CT, Alfidi RJ, Kaufman B, Levin M. Magnetic resonance imaging of the orbit: a preliminary experience. *Radiology* **1984**;150:755–759
21. Axel L. Surface coil magnetic resonance imaging. *J Comput Assist Tomogr* **1984**;8:381–384